ENERGY LOSS DUE TO IRRADIANCE ENHANCEMENT

Mike Zehner[(1)], Toni Weigl[(1)], Matthias Hartmann[(1)], Stefan Thaler[(1)], Oliver Schrank[(1)]
Moritz Czakalla[(1)], Bernhard Mayer[(2)], Thomas R. Betts[(3)], Ralph Gottschalg[(3)], Klaus Behrens[(4)]
Gert König Langlo[(5)], Bodo Giesler[(6)], Gerd Becker[(1)], Oliver Mayer[(7)]

[(1)]Munich University of Applied Sciences, Department of Electrical Engineering, Degree Program Renewable Energies - Working Group of the Solar Technology Lab, 80323 München, Germany
Phone: +49 (0) 89 1265-4412, Fax: +49 (0) 89 1265-3403, mike.zehner@hm.edu

[(2)]Ludwig-Maximilians-Universität Munich, Chair of Experimental Meteorology, Theresienstraße 37, 80333 Munich, Germany

[(3)]Centre for Renewable Energy Systems Technology (CREST), Department of Electronic and Electrical Engineering, Loughborough University, United Kingdom

[(4)]Deutscher Wetterdienst, Lindenberg Meteorological Observatory, Richard-Aßmann-Observatory OT Lindenberg Am Observatorium 12, 15848 Tauche, Germany

[(5)]Alfred Wegener Institute for Polar and Marine Research Am Handelshafen 12, 27570 Bremerhaven, Germany

[(6)]Siemens AG, Würzburger Straße 121, 90766 Fürth, Germany

[(7)]GE Global Research, Freisinger Landstraße 50, 85748 Garching, Germany

ABSTRACT The analysis of high resolution measurement data from Munich showed significant and repeated irradiance peaks. For irradiance enhancement (IE), the observed irradiance is above the theoretically-calculated global irradiance of a clear-sky day (i.e. for the given time with a clear-sky and atmosphere). The increased irradiance is caused mainly by reflections from cumulus clouds. Concurrent with the elevated global irradiance, low ambient and module temperatures were observed, due to cloud coverage between irradiance enhancement peaks. This analysis investigates the essential meteorological observations from these data records. It also depicts the technological effects on a PV system. To illustrate this, the irradiance peaks are classified by their specific characteristics such as magnitude, duration, distribution or slope. Data sets from several Baseline Surface Radiation Network (BSRN) sites, representing various climatic zones are examined to evaluate the magnitude of this effect across Europe and its dependence on general meteorological conditions. It is crucial to understand the PV system response to the monitored IE-effects. The employment of the simulation environment INSEL (for various PV cell types and panels) enables simulations incorporating high resolution measurement data and (commercially available) PV module simulation data. The output power of the modules investigated can be up to 30 % higher than under STC conditions. The system response was also explored by using a solar generator simulator and by evaluating data sets of operating MW PV plants.

Keywords: Irradiance Enhancement Effect, Modelling, Solar Radiation, Sizing Ratio, System Performance

1 Goals and Motivation

The analysis of highly accurate sets of measurement data from Munich, clearly show recurring irradiance peaks [1]. These irradiance enhancements feature a radiation density above the theoretical values calculated for a clear-sky day. The enhanced values for global irradiance mainly originate from the reflections of light waves from cumulus clouds. These clouds appear as isolated, consistently thick clouds forming cotton-wool shapes in the vertical plane. In most cases the clouds hover below the freezing point and consist mainly of water droplets, so that their flanks are clearly distinguished from the background. The clouds' clear contours enable the reflection of the irradiance, implying additional localised input leading to the irradiance enhancement (IE) effect. Due to the low velocity with which the clouds pass, for example Munich, the IE effect can persist for up to several minutes. Another phenomenon correlating with the irradiance enhancement peaks is the lower module temperature. On IE-days the module temperature was clearly below the temperature measured on a clear-sky day (shorter energy input, inert thermal mass of the module and lower ambient temperature). These findings have been expanded upon and complemented with a broader analysis of highly accurate measurement data from several Baseline Surface Radiation Network (BSRN) locations across Europe being representative for certain climatic zones [2], [3]. This improves the previous statements and confers a better universal validity. Considerations upon the system response to IE are shown on the basis of selected exemplary work results.

2 Irradiance Enhancement (IE) – Cause and Effect

The weather conditions leading to the perceived excessive increase of the radiation density are common but often not consciously perceived. Figures 1a to 1d show snapshots of a generic IE reference day (Munich, July 8th '09) where banks of cumulous clouds are shaping up in parallel to the wind direction. Figure 2 illustrates the effect the IE has by monitoring the radiation density during the course of another IE reference day (Munich, May 30th '09). The course of the irradiance (in red) is offset against the clear-sky day calculated with the software libRadtran[1] [4]. The additional energy input, conditioned by the peaks of the irradiance enhancements is shown in purple.

[1] libRadtran - library for radiative transfer, www.libradtran.org

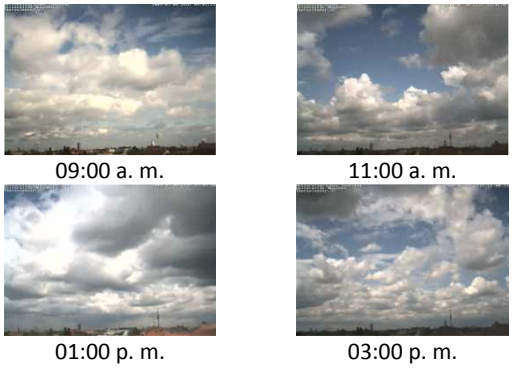

Figure 1a to 1d: Snapshots of various weather situations throughout the course of the generic IE reference day (July 8th 2009) recorded in Munich [5].

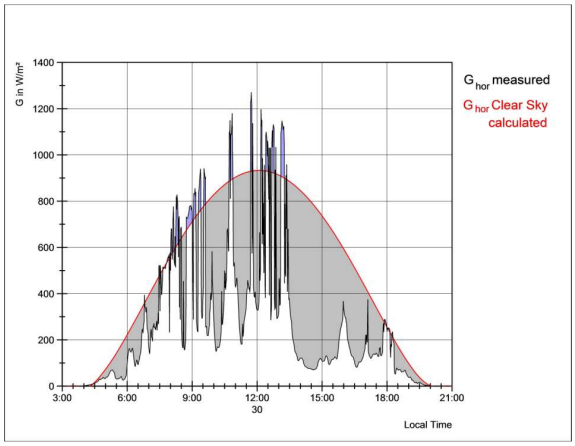

Figure 2: Course of the global radiation (black) throughout the day for a further reference IE-day (May 30th 2009). The red graph shows the profile of the calculated clear-sky day. The energy input conditioned by the peaks of the irradiance enhancements is displayed in purple.

3 IE – Data Mining: Analysis of highly accurate measurement data sets

In Germany the data accumulation from Munich was complemented with data sets from the Baseline Surface Radiation Network (BSRN) [2]. There were several specific reasons for choosing the BSRN data sets as the basis for further evaluation. The recording of the BSRN data sets has a resolution of one mean value per minute. This is not ideal still, much better compared to the resolutions of other data sets otherwise available from PV systems. Besides that, the accuracy of the BSRN data sets is an important feature. The data sets are based upon three matching reference sensors. Measured values are averaged and deviations are denominated. Data availability is another important issue. The BSRN data sets contain over several years data from 40 stations worldwide. So the evaluation performed for Europe could be expanded to America and the Far East. Reliability is further important consideration. The BSRN sensors are cyclically revised and maintained. One last factor is the traceability of the measured values: All the BSRN sensors have valid calibration certificates. The European database enlargement of this evaluation aims at covering as many of the European climatic zones as possible [3].

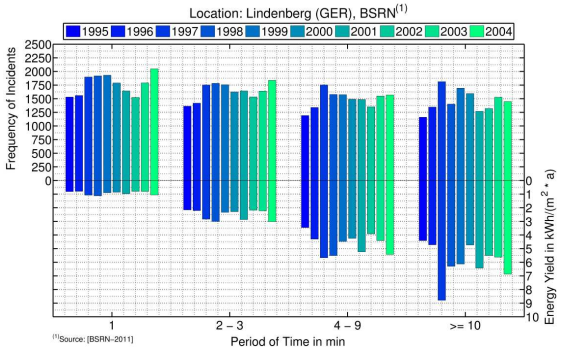

Figure 3: Frequency and energy content of IE, classified according to duration of the IE events, for the years 1995 to 2004. Measured at OT Lindenberg (Germany).

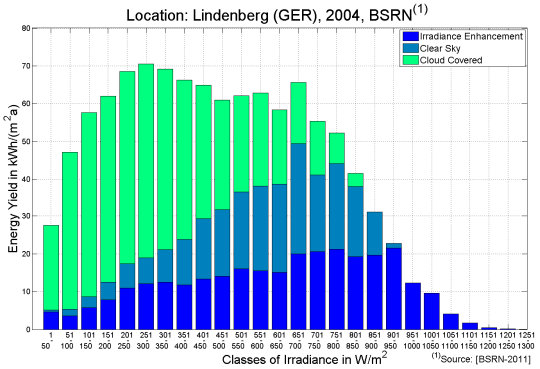

Figure 4: Classification according to the performance of the radiation density and associated energy yield. The final yield under different weather conditions is displayed in % providing performance fractions (Cf. [6]).

As an exemplary BSRN-site the Lindenberg observatory near Berlin (Germany) was chosen. Besides the measured values, synoptic information was also recorded. Figure 3 illustrates the relevance of the IE incidents by describing their duration, frequency and the energy content. According to the duration of each IE event, the values were classified into the time-ranges displayed on the x-axis. The upper left y-axis indicates the frequency of the events for each year. The energy content of the bins is shown by the lower right y-axis in kWh/(m²a). This shows the energy contribution above the clear-sky case. The energy yield at IE conditions shows that the energy fraction above the theoretical clear-sky (CS) averaged over 10 years represents 1.58 % of the final energy yield of the site. The integral of the absolute values of the IE incidents averaged over 10 years, results in 25.3 % of the final yield of the site. Figure 4 shows the energy as a percentage of the final yield and assigned to different weather conditions at Lindenberg in 2004.

Table 1: IE data mining – data record 1 (Europe)

No.	Site	Country	Source	Climatic Zone
1	Lerwick	GB	BSRN	II-1
2	Camborne	GB	BSRN	III-2
3	Lindenberg	DE	BSRN	III-3
4	Munich I	DE	PV	III-3
5	Munich II	DE	MI	III-3
6	Toravere	EE	BSRN	III-4
7	Carpentras	FR	BSRN	IV-1 and IV-2

Table 1 gives a survey of the chosen and representative BSRN locations and their mapping to certain climatic zones. Figure 5 shows the IE impact in average values for these locations from 1995 to 2004.

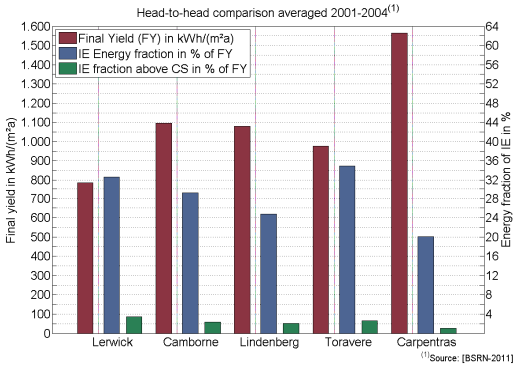

Figure 5: Site Assessment - 5 representative European BSRN Locations in comparison.

The y-axis located on the left side displays the mean values for final energy yield. The second y-axis at the right shows the energy generated at IE conditions as the percentage of the FY. The third value denominates the energy part above the theoretical clear-sky curve.

4 IE – Considerations upon the System Response

The following calculations and analysis for the simulation of the PV modules are based on two data sets measured at the MW-plant on the Munich trade fair [7]. Both reference days chosen for this analysis show the characteristic profiles for summer weather with according irradiance and temperature courses. The course of July 27th 2009 shows the particular characteristics of a clear-sky (CS) day, while July 8th 2009 was picked as an IE-day with fluctuations of the radiation density. The application of the modular simulation language INSEL[2] is a well-founded and validated basis to model a PV system and perform different parameter variations. The module utilized was chosen from a range of customary PV modules with various structures. Only the results for the calculations with the mono-crystalline module (mc) are being presented here.

Figure 6a (top) displays the CS reference day and 6b (bottom) shows the IE reference day. The figures display the course of the ambient and module temperatures for both reference days. On the CS day the values of the module temperature display a typical hysteresis loop. The figures illustrate the operating values of a typical mc-module on both reference days. Located on the bottom are the system values: voltage in blue, current in black and power in purple, all normalized to the STC values and displayed against the irradiance. The current is not only normalized to STC but also divided by the momentary horizontal global irradiance in order to illustrate the proportionality. Two auxiliary lines are plotted in the figures in light grey. The increasing angle bisector equals the ideal power which increases proportionally to the irradiance. The line at the value 1 should ideally be identical with the normalized voltage and the current. On the CS day just two thirds of the figure's width was used due to the lower irradiance. The charts depict the influence of the two input parameters radiation density and module temperature convincingly.

[2] INSEL 8.0.1, Doppelintegral GmbH, www.insel.eu

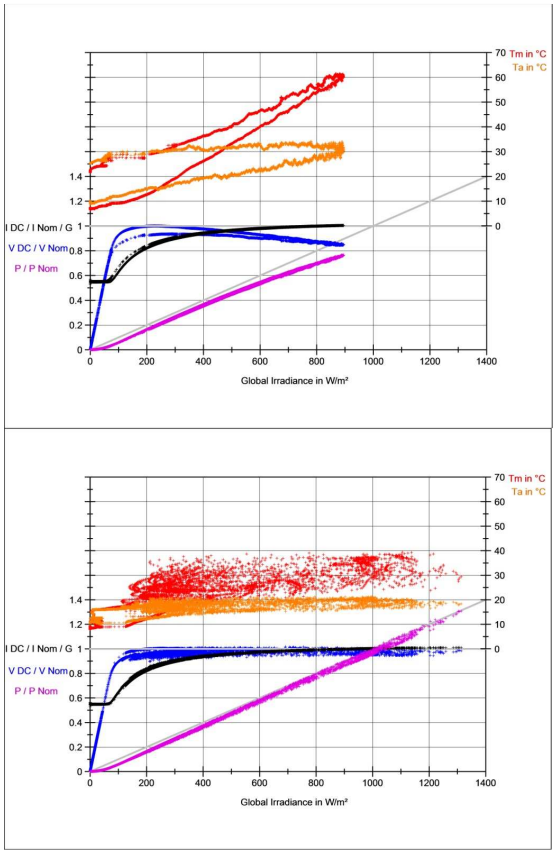

Figure 6a, b: The upper (CS) and the lower (IE) chart give a comparison of the electrical key values on the two reference days including the ambient temperature as input parameter for the modelling (cf. [8]).

The scatter plot in figure 7 displays the standardised courses of power and current against the voltage for the mc-module. Lighter dots indicate the CS day and darker dots the IE day. On IE days, the module temperatures stay at almost constant levels. Therefore the voltage for the crystalline modules also stays relatively constant on those days. The voltage remains in the region around 0.95 to 1 times the STC MPP voltage. The current and power curves on the CS day bend significantly towards the y-axis due to the decreasing voltage. The MPP voltage falls to 85 % of the STC value. With a current max. at 90 % of the STC value and a max. irradiance of 893 W/m² (compared to 130 % on IE) the current on IE days is clearly above the CS day's current.

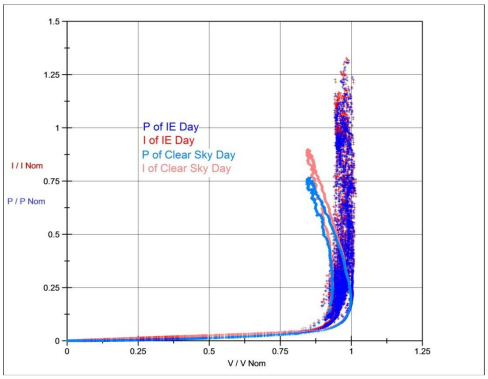

Figure 7: The scatter plot shows the course of the standardised values of current (in red) and power (in blue) over voltage for the CS day (in lighter colours) and the IE day (in darker colours) for a mc-module.

For the IE-day the power peaks almost to the values of the current. This means that the module also has about 30 % more power than under STC. This module has a nominal power rating of 170 W corresponding to additional 51 W of power for every module in a PV plant. The comparison is depicted in figure 8, illustrating the normalized power output of the clear-sky day (in blue) and that of the IE day (in red) for the mc-module. The peak MPP of the IE day is about 67 % higher than the MPP of the CS day. This value is identical for other investigated modules. The efficiency under IE conditions is higher than on a CS day, almost all day long.

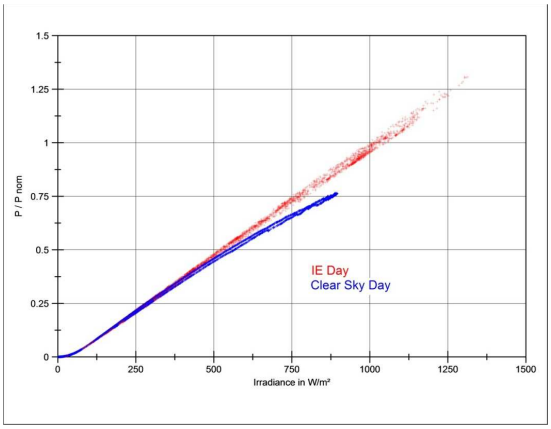

Figure 8: The figure displays a comparison between the normalized power output of an mc-module of the CS (IE) day in blue (in red) over the range of irradiance values

Figure 9 shows example results from the studies on the IE system response. An IE Test Profile was developed, which should picture the characteristics of IE incidents. Several test runs were defined for an experimental set-up with a solar generator simulator and several commercially available inverters representing different inverter topologies. The four charts of figure 9 show an example test run with one inverter for the IE test profile and the sizing ratios ($P_{PV\text{-}STC}/P_{INV\text{-}Max}$) 0.83, 1.0, 1.11 and 1.25 [9]. The target values of the solar generator are indicated in dark red. The power dissipation curve is visible in black. The target-actual comparison shows the MPP-tracking at IE conditions (in dark blue and light red) plotted for several sizing ratios. Further work results such as the evaluation of operating data sets are shown in [10].

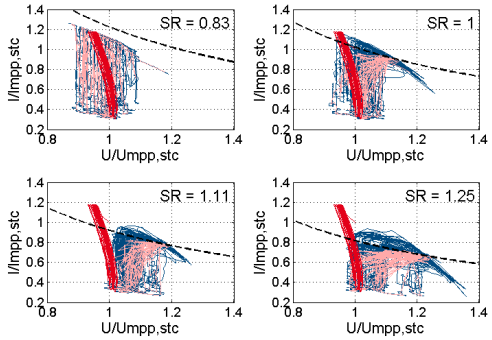

Figure 9: The four charts show simulation results with thin film modules and an example commercially available inverter for an IE test profile and several sizing ratios (0.83, 1.0, 1.11, and 1.25). The target (in dark red) actual (in blue and light red) comparison shows the quality of the MPP-tracking under IE conditions.

5 SUMMARY AND OUTLOOK

All analysed sets of highly accurate meteorological measurement data convincingly depict the irradiance enhancement. At Lindenberg (Germany) the energy yield under IE conditions shows that the energy fraction above the theoretical CS averages 1.58 % of the final energy yield. The integral of the absolute values of the IE incidents averages 25.3 % of the final yield at the site. The perceived incidents could be verified by all sites studied throughout Europe. The enhancements are typically related to low module temperatures and induce the corresponding peaks of the module MPP-power. Calculations with the simulation language INSEL revealed a power output of up to 1.3 times higher than the nominal power of crystalline PV modules.

First studies on the system response indicate that the IE effects have an important impact on the operating behavior of PV systems. Irradiance enhancements affect the power output of photovoltaic systems, even more clearly as a function of the sizing ratio.

6 REFERENCES

[1] Zehner M., Weigl T., Weizenbeck J., Mayer B., Wirth G., Prochaska H., Giesler B., Gottschalg R., Becker G., Mayer O., Systematische Untersuchung meteorologischer Einstrahlungsereignisse, 25th PV-Symposium, Staffelstein (Germany), 2010

[2] WRMC-BSRN (World Radiation Monitoring Center – Baseline Surface Radiation Network), www.bsrn.awi.de.

[3] Troll, C. & Paffen, K. (1964).- Die Jahres-zeitenklimate der Erde. (Summary: The seasonal climates of the Earth). Erdkunde 18: 1-28 + map

[4] Mayer B., Kylling, A., The libRadtran software package for radiative transfer calculations: Description and examples of use, journal acp, 5/05,

[5] Meteorological Institute, Ludwig-Maximilians-University Munich, data records for the years 2008 and 2009, weather observation films, www.meteo.physik.uni-muenchen.de

[6] Haselhuhn R., Energy Rating of PV modules, DKE Workshop, Intersolar Munich 2011.

[7] Bavarian Association for the Promotion of Solar Energy, data records of the PV plant New Munich Trade Fair for 2008 and 2009, www.sev-bayern.de

[8] Ransome S., A Summary of 6 years performance modelling from 100+ sites worldwide, 31st IEEE PVSC, Orlando (USA), 2005.

[9] Burger B., Rüther R., Inverter sizing of grid-connected photovoltaic systems in the light of local solar resource distribution characteristics and temperature, Solar Energy 80 (2006) 32–45

[10] Giesler B, et al., Operating data analysis of various subsystems at the 20 MW PV plant Rothenburg, 26th EU PVSC, Hamburg (Germany), 2011.

7 DEFINITIONS

Table 2: Definitions and graph colours used of measured and normalized parameters [6].

No.	*Abbr.*	Formula	Comment
1	*V*	$V_{DC.MPP}/V_{Nom}$	Normalized DC voltage
2	*I*	$I_{DC.MPP}/(I_{nom} \times G)$	Normalized DC current
3	*P*	$P_{DC.MPP}/P_{Nom}$	Normalized DC power